

Co-Teaching for Unsupervised Domain Adaptation and Expansion

Kaibin Tian, Qijie Wei, Xirong Li

Key Lab of DEKE, Renmin University of China
Vistel AI Lab

Abstract. Unsupervised Domain Adaptation (UDA) is known to trade a model’s performance on a source domain for improving its performance on a target domain. To resolve the issue, Unsupervised Domain Expansion (UDE) has been proposed recently to adapt the model for the target domain as UDA does, and in the meantime maintain its performance on the source domain. For both UDA and UDE, a model tailored to a given domain, let it be the source or the target domain, is assumed to well handle samples from the given domain. We question the assumption by reporting the existence of cross-domain visual ambiguity: Due to the lack of a crystallly clear boundary between the two domains, samples from one domain can be visually close to the other domain. We exploit this finding, and accordingly propose in this paper *Co-Teaching* (CT) that consists of knowledge distillation based CT (kdCT) and mixup based CT (miCT). Specifically, kdCT transfers knowledge from a leader-teacher network and an assistant-teacher network to a student network, so the cross-domain visual ambiguity will be better handled by the student. Meanwhile, miCT further enhances the generalization ability of the student. Comprehensive experiments on two image-classification benchmarks and two driving-scene-segmentation benchmarks justify the viability of the proposed method.

Keywords: UDA, UDE, Co-Teaching, Knowledge Distillation

1 Introduction

Unsupervised Domain Adaptation (UDA), aiming to adapt a model trained on a *labeled* source domain for an *unlabeled* target domain without the need of re-labeling any data, is a crucial technique for real-world AI [2, 18, 19]. Applications of this technique includes cross-view person re-ID [13, 45], cross-device medical image analysis [27, 40], and cross-condition autopilot scene segmentation [24, 34], to name just a few. Thanks to the advent of novel methods for UDA [31, 41], we witness an ever-growing performance on the target domain, as demonstrated by public benchmark evaluations such as Office-Home [35] and DomainNet [21] for multi-class image classification and ACDC [25] for driving scene segmentation. However, it has been documented recently in the context of image classification that UDA in fact trades the model’s performance on the source domain for

improving its performance on the target domain [37, 39]. Such a finding is disturbing, as it suggests that one may have to deploy simultaneously two models to support both domains. Even putting the doubled deployment cost aside, how to swiftly switch between the models is nontrivial as from which domain a test sample comes is unknown. The degeneration of the source-domain performance puts the real-world applicability of UDA into question.

To remedy the issue, GSFDA [39] resorts to continual learning to preserve a model’s ability on the source domain while being adapted to the target domain. Since the method assumes zero availability of the original samples from the source domain, it has little chance to recover once degeneration occurs. Indeed, our evaluation indicates that GSFDA remains suffering performance loss on the source domain.

To explicitly quantify the issue, a variant of UDA termed Unsupervised Domain Expansion (UDE) is introduced by [37]. UDE has the same starting point as UDA, *i.e.* a set of *labeled* samples from the source domain and a set of *unlabeled* samples from the target domain. The difference is that the evaluation protocol of UDE reports the performance on the source domain and consequently the performance on an expanded domain covering both the source and target domains. Besides, [37] proposes a new method called KDDE. This method assumes that a model tailored to a given domain, let it be the source or the target domain, can well handle samples from the given domain. Accordingly, KDDE runs in two steps, where two domain-specific models are first trained for the source and target domains, respectively. It then performs knowledge distillation, where the dark knowledge of the source-specific (target-specific) teacher is transferred to a student model via source-domain (target-domain) samples exclusively.

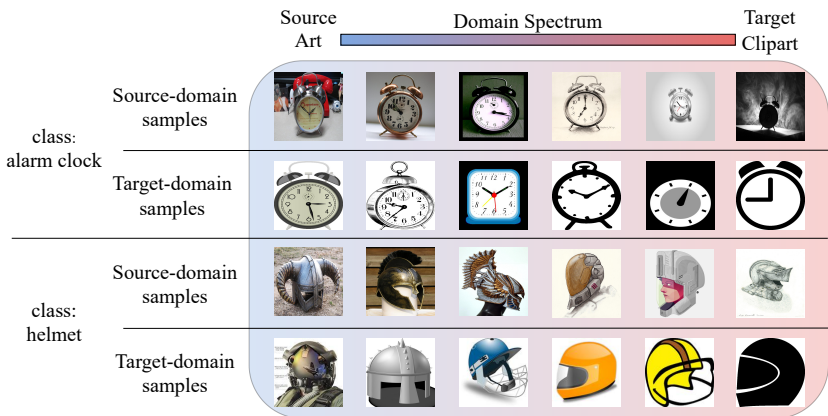


Fig. 1. Illustration of cross-domain visual ambiguity. Samples from a target domain (*Clipart*) can be visually realistic as samples from a source domain (*Art*), and vice versa. This points out an overlooked fact that there lacks a crystally clear boundary between the source and target domains. Data from Office-Home [35].

We question the assumption of [37] by reporting the existence of cross-domain visual ambiguity. As exemplified in Fig. 1, while the source and target domains are known to be distinct, there lacks a crystallly boundary between the two. Hence, samples from one domain can be visually close to the other domain. As such sorts of samples are in minority in their host domain, they tend to be overlooked by the domain-specific model. However, they are likely to be better handled by the model targeted at the other domain. Departing from this observation, we propose in this paper Co-Teaching (CT) which exploits the domain-specific models in a more effective manner for UDA and UDE. In particular, our major contributions are as follows:

- We propose Co-Teaching (CT) as a generic method for unsupervised domain adaptation and expansion. CT consists of knowledge distillation based CT (kdCT) and mixup based CT (miCT). Specifically, kdCT transfers knowledge from a leader-teacher network and an assistant-teacher network to a student network, to let the student better resolve cross-domain visual ambiguity, while miCT further enhances the generalization ability of the student.
- Comprehensive experiments on two image-classification benchmarks, *i.e.* Office-Home [35] and DomainNet [21], and two driving-scene-segmentation benchmarks, *i.e.* Cityscapes [4] and ACDC [25], justify the viability of the proposed method and its superior performance against competitive baselines.

2 Related Work

Progress on UDA. The major line of research on UDA is to learn domain-invariant feature representations, either by domain discrepancy reduction [11, 15, 30, 33] or by adversarial training [6, 12, 14, 23, 43]. In Deep Domain Confusion (DDC) [33], the domain discrepancy between features from the source / target domains is defined as the maximum mean discrepancy (MMD) on the last layers of a deep image classification network. Contrastive Adaptation Network (CAN) [11] takes class information into account, measuring both intra-class and inter-class domain discrepancy. Domain Adversarial Neural Network (DANN) [6] is among the first to introduce adversarial training into the context of UDA. CDAN [14] extends DANN by taking the multiplicative interaction of feature representations and class predictions as the input of its discriminator. SRDC [31] enhances its discriminator by clustering features from intermediate layers of the network. All the above is conducted for image classification.

We notice an increasing interest in extending UDA from the image level to the pixel level for cross-domain semantic image segmentation. AdaSegNet [32] and Advent [36] use adversarial training at the output space, while pixel-level adaptation is performed in DCAN [38] and Cycada [10]. The state-of-the-art FDA [41] uses self-predicted pseudo labels for self-supervised training.

Our proposed CT method conceptually differs from the existing works as it essentially performs meta learning on top of a specific UDA method. Moreover, in contrast to the prior art which cares only the target-domain performance,

CT aims for a broader scope that covers the source and target domains both. While GSFDA [39] tries to prevent performance deterioration on the source domain by continual learning, while PDA [16] attempts to balance the source supervised loss and the cross-domain alignment loss by Pareto optimal solution. Our experiment indicates that the deterioration remains. CT works better for both image classification and semantic segmentation.

Progress on UDE. CT is inline with KDDE [37], as both aim for training a model that suits the expanded domain by knowledge distillation (KD). However, KDDE uses its teacher networks in a relatively limited manner, where the knowledge of the teacher network trained for the source (target) domain is transferred to the student network via the source (target) samples exclusively. Consequently, KDDE lacks the ability to exploit the potential of the teacher network derived from one domain in handling cross-domain visual ambiguity for the other domain.

Multi-Teacher Knowledge Distillation (MTKD). MTKD has been used in the context of multi-source UDA, where multiple domain-adapted teacher models are trained by pairing the target domain with each of the multiple source domains [1, 26]. Such a tactic is inapplicable to single-source UDA as this paper works on. In the context of standard supervised learning, MultiT [42] transfers the dark knowledge of multiple pre-trained teacher networks to a student network by minimizing the KL divergence between the averaged prediction of the teachers and the prediction of the student. Treating the teachers equally, MultiT is suboptimal for UDA/UDE.

Co-Teaching. It is worth pointing out that the term co-teaching has been used in other contexts which conceptually and technically differ from ours. For supervised learning, Decoupling [17] and Co-Teach [7] aim for label denoising within a single domain. Decoupling simultaneously trains two models h_1 and h_2 , updating them with samples having $h_1(x) \neq h_2(x)$ in a given mini-batch. Co-Teach alternately uses samples correctly classified by one model to train the other model. Since both methods are fully supervised, they are inapplicable for UDA/UDE where the target domain is unlabeled. For multi-target domain adaptation, CGCT [22] proposes a co-teaching strategy that uses a dual classifier head to provide pseudo labels for unlabeled target-domain samples. As our Co-Teaching is model-agnostic, any UDA method including CGCT can in principle be used to instantiate the UDA module of our method.

3 Proposed Co-Teaching Method

3.1 Problem Formalization

We use x to indicate a specific sample. For a manually labeled sample, we use y to indicate its manual annotation, which can be a one-hot vector for multi-class image classification or a multi-dimensional binary mask for semantic image segmentation. Let \mathcal{N} be a deep neural network, which is supposed to output $\mathcal{N}(x)$ that well matches the (unknown) label of a novel sample. Following [37],

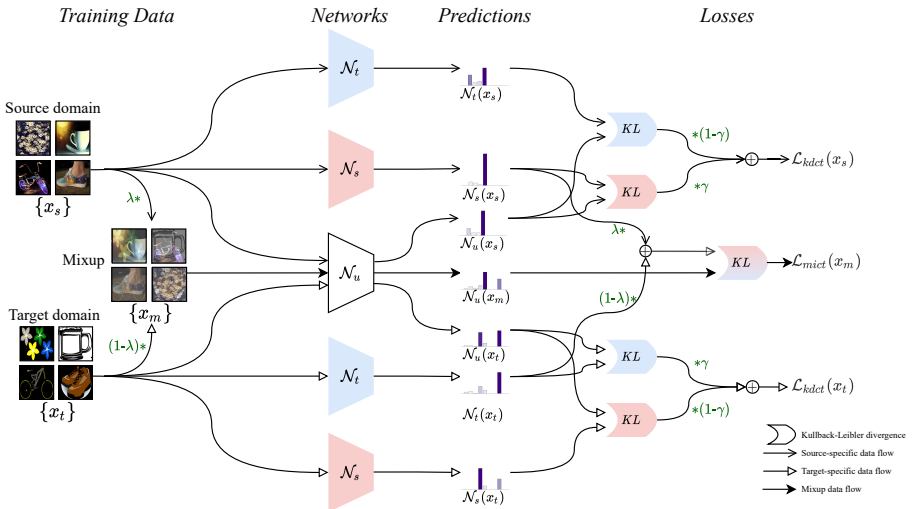


Fig. 2. Proposed Co-Teaching (CT) method for unsupervised domain adaptation and expansion. Given a set of labeled samples $\{(x_s, y_s)\}$ from a source domain and unlabeled data $\{x_t\}$ from a target domain, CT obtains a *domain-expanded* network \mathcal{N}_u by two-stage training. In the first stage, two *domain-specific* teacher networks \mathcal{N}_s and \mathcal{N}_t are obtained, where \mathcal{N}_s for the source domain is trained on $\{(x_s, y_s)\}$ by standard supervised learning, whilst \mathcal{N}_t for the target domain is trained on $\{(x_s, y_s)\}$ and $\{x_t\}$ by an existing UDA method. In the second stage, \mathcal{N}_s and \mathcal{N}_t are used in a cooperative manner to teach \mathcal{N}_u , achieved by 1) **knowledge distillation based CT** (kdCT) that minimizes $L_{kdct}(\{x_s\}) + L_{kdct}(\{x_t\})$, and 2) **mixup based CT** (miCT), minimizing $L_{mict}(\{x_m\})$ for mixup instances $\{x_m\}$. Once trained, only \mathcal{N}_u is needed for inference. CT works for distinct tasks including image classification and semantic image segmentation.

we formalize the UDE task as follows. Given a set of n_s *labeled* samples $\{(x_s, y_s)\}$ randomly sampled from a source domain D_s and a set of n_t *unlabeled* samples $\{x_t\}$ sampled randomly from a target domain D_t , the goal of UDE is to train \mathcal{N} that works for an expanded domain covering both D_s and D_t . Accordingly, we use D_{s+t} to indicate the expanded domain.

The previous approach to UDE, as aforementioned, is Knowledge Distillation Domain Expansion (KDDE) [37]. At a high level, KDDE works in two stages. In the first stage, two domain-specific teacher networks \mathcal{N}_s and \mathcal{N}_t are trained, where \mathcal{N}_s for D_s is learned from the labeled set $\{(x_s, y_s)\}$ by standard supervised learning, while \mathcal{N}_t for D_t is trained on $\{(x_s, y_s)\}$ and $\{x_t\}$ by an off-the-shelf UDA method. In the second stage, knowledge distillation (KD) is performed to inject the dark knowledge of the teacher networks into a student network \mathcal{N}_u , which will be eventually used for inference. Depending on the domain identity of

a training sample, KDDE selectively uses the two teachers, *i.e.* \mathcal{N}_s to deal with samples from D_s and \mathcal{N}_t for samples from D_t , see Eq. Eq. (1).

$$\begin{cases} \mathcal{N}_s \leftarrow \text{supervised-learning}(\{(x_s, y_s)\}) \\ \mathcal{N}_t \leftarrow \text{UDA}(\{(x_s, y_s)\}, \{x_t\}) \\ \mathcal{N}_u \leftarrow \begin{cases} \text{KD}(\mathcal{N}_s, \{x\}), & x \in D_s \\ \text{KD}(\mathcal{N}_t, \{x\}), & x \in D_t \end{cases} \end{cases} \quad (1)$$

The two-stage property of KDDE ensures flexibility in choosing UDA methods for implementing \mathcal{N}_t . We therefore opt to inherit this property, but introduce a novel Co-Teaching (CT) method into the second stage.

3.2 Framework

As illustrated in Fig. Fig. 2, CT consists of knowledge distillation based CT (kdCT) and mixup based CT (miCT). Both kdCT and miCT are introduced to exploit the domain-specific advantages of the two teacher networks. In particular, kdCT allows the student network to simultaneously learn the two teacher networks' dark knowledge about every training sample. Meanwhile, miCT improves the generalization ability of the student network by using the mixup technique in a cross-domain manner. As the two implementations of CT are orthogonal to each other, they can be used either alone or jointly.

3.2.1 Knowledge Distillation based Co-Teaching We depart from a standard KD process with one student network (\mathcal{N}_u) and one teacher network, either \mathcal{N}_s or \mathcal{N}_t . Let us consider \mathcal{N}_s for instance. Given a set of samples $\{x\}$, KD from \mathcal{N}_s to \mathcal{N}_u is achieved by minimizing the Kullback-Leibler (KL) divergence between $\mathcal{N}_s(\{x\})$ and $\mathcal{N}_u(\{x\})$, defined as $KL(\mathcal{N}_s(\{x\}), \mathcal{N}_u(\{x\}))$. In a similar manner, we define the loss of KD from \mathcal{N}_t to \mathcal{N}_u $KL(\mathcal{N}_t(\{x\}), \mathcal{N}_u(\{x\}))$. To perform multi-teacher KD, a straightforward solution is to average the two losses. In the context of UDA / UDE, however, the two teacher networks are supposed to specialize in handling samples from their targeted domains. Therefore, we shall not treat them equally. To be more precise, for training samples from D_s , we expect that \mathcal{N}_s leads the teaching process, while the \mathcal{N}_t acts as an assistant. The opposite is true when exploiting training examples from D_t . To that end, we introduce a parameter γ to weigh the importance of two teachers in the kdCT process as:

$$L_{kdct}(\{x\}) = \begin{cases} \gamma \cdot KL(\mathcal{N}_s, \mathcal{N}_u) + (1 - \gamma) \cdot KL(\mathcal{N}_t, \mathcal{N}_u) & x \in D_s \\ \gamma \cdot KL(\mathcal{N}_t, \mathcal{N}_u) + (1 - \gamma) \cdot KL(\mathcal{N}_s, \mathcal{N}_u) & x \in D_t \end{cases} \quad (2)$$

Given Eq. (2), KDDE can now be viewed as a special case of kdCT with $\gamma = 1$. Such a mechanism provides the *possibility* of making correct decision for the samples, which subjectively divided into the host domain but have more opposite domain styles. By contrast, KDDE, exclusively using one teacher network for one domain, lacks such a compensation mechanism by definition.

Concerning the choice of γ , in principle we shall a value larger than 0.5 to emphasize the leading-teacher network, which is \mathcal{N}_s for samples from D_s and \mathcal{N}_t for samples from D_t . It has been recognized that introducing certain randomness into the process of deep network training can make the network more resistant to noise and thus improve its robustness [5, 9, 29, 44]. Therefore, we let γ follow a probability distribution, instead of using a fixed value. Since the beta distribution can produce diversified probability distributions with ease by adjusting two positive shape parameters denoted by α and β , we choose to use $\gamma \sim \text{Beta}(\alpha, \beta)$. Our randomness is introduced at a mini-batch level, by sampling randomly a specific γ from the beta distribution per batch.

Given the two domain-specific losses $L_{kdct}(\{x_s\})$ and $L_{kdct}(\{x_t\})$ computed by Eq. (2), we define the overall loss L_{kdct} as their sum.

3.2.2 Mixup based Co-Teaching The Mixup technique [44], which synthesizes a new training sample by a convex combination of two real samples, is shown to be effective for improving image classification networks. We thus repurpose this technique to generate new domain-expanded samples denoted by $\{x_m\}$. In particular, x_m is obtained by blending x_s randomly chosen from D_s with x_t randomly chosen from D_t .

Our mixup based Co-Teaching (miCT) is implemented by transferring the two-teacher knowledge via the mixed samples to the student network. The teachers’ joint knowledge w.r.t. x_m is naturally reflected by their combined prediction denoted as \hat{y}_m . Accordingly, the loss of miCT L_{mict} is computed as

$$\begin{cases} x_m &= \lambda \cdot x_s + (1 - \lambda) \cdot x_t, \\ \hat{y}_m &= \lambda \cdot \mathcal{N}_s(\{x_s\}) + (1 - \lambda) \cdot \mathcal{N}_t(\{x_t\}), \\ L_{mict} &= KL(\hat{y}_m, \mathcal{N}_u(\{x_m\})). \end{cases} \quad (3)$$

with $\lambda \sim \text{Beta}(1, 1)$.

Both L_{kdct} and L_{mict} are KL-divergence based losses for knowledge distillation. So they can be directly added and minimized together for the joint use of kdCT and miCT.

3.3 Applications

As Fig. 2 shows, CT is a generic method for UDA and UDE. Depending on the choice of the network and the loss function, the method can be used with ease for multi-class image classification and semantic image segmentation. For the former task, a classification network, *e.g.* ResNet [8], shall be used with the KD losses computed at the image level. For the latter, a segmentation network, *e.g.* DeepLabv2 [3], shall be adopted with the KD losses computed at the pixel level.

4 Experiments

We evaluate the viability of the proposed CT method in the context of two tasks, *i.e.* multi-class image classification and driving scene segmentation. It is worth

pointing out that UDE as an emerging topic is less studied. We shall naturally include methods directly targeted at UDE, namely KDDE [37]. Meanwhile, as our method is built based on two teacher networks (\mathcal{N}_s and \mathcal{N}_t), methods used for obtaining these networks, *e.g.* SRDC for image classification [31] and FDA [41] for semantic segmentation, shall be treated as baselines. In addition, methods developed for other purposes yet technically applicable for UDE, *e.g.* MultiT [42] which performs knowledge distillation given multiple teachers is also included. So for a fair and comprehensive evaluation, we organize the competitor methods into the following three groups: methods targeted at UDE, methods targeted at UDA, and methods technically related. All experiments are run within the PyTorch framework with two NVIDIA Tesla P40 cards.

4.1 Task 1. Multi-Class Image Classification

4.1.1 Experimental Setup We adopt two public collections, Office-Home [35] and DomainNet [21]. Office-Home contains 15,588 images of 65 object classes common in office and home scenes, *e.g.* chair, table and TV. There are four different domains, *i.e.* artistic images (A), clip art (C), product images (P), and real-world images (R). DomainNet, previously used in the Visual Domain Adaptation Challenge at ICCV 2019¹, has 362,470 images of 345 object classes from four domains, *i.e.* clipart, painting, real, and sketch. In order to evaluate a model’s performance on both source and target domains, we adopt the data split provided by [37], where images per domain have been divided at random into two disjoint subsets, one for training and the other for test². A specific UDE task is defined with one domain as D_s and another domain as D_t . Per collection, by pairing its individual domains, we define 12 tasks in total.

Competitor methods. We include as a baseline ResNet-50 trained by standard supervised learning on D_s . As mentioned above, we compare with existing methods from the following three groups:

- Method targeted at UDE: KDDE [37].
- Methods targeted at UDA: DDC [33], DANN [6], DAAN [43], CDAN [14], SRDC [31], PDA [16] and GSFDA [39].
- Method technically related: MultiT [42].

As each method is provided with the same training data and eventually yields a specific ResNet-50 network for inference, such an experimental setup enables a head-to-head comparison between the different methods.

Details of implementation. Following [37], we train networks by SGD with a momentum of 0.9, an initial learning rate of 0.005, and a weight decay of 0.0005. The learning rate is decayed by 0.1 every 30 epochs on Office-Home and every 10 epochs on DomainNet. A fixed number of training epochs is used, which is 100 for Office-Home (with batch size 32) and 30 on DomainNet (with batch size 96) as the latter is much larger. Models obtained at the last epoch are

¹ <http://ai.bu.edu/visda-2019>

² <https://github.com/li-xirong/ude>

used for evaluation. Each method is run independently three times with averaged performance reported.

Performance metric. We report accuracy (%), *i.e.* the percentage of test images correctly classified.

4.1.2 Results on Office-Home Tab. 1 shows the performance of the different methods on the source (D_s), target (D_t) and expanded (D_{s+t}) domains, respectively. The UDA method consistently show performance degeneration on D_s . Even though GSFDA is meant for maintaining a model’s performance on D_s , it suffers from a performance drop of 2.53% (from 82.43 to 79.90). Among the three UDE methods, the proposed CT performs the best. Given DDC as \mathcal{N}_t , CT even outperforms \mathcal{N}_s on D_s . When evaluated in the UDA setting to which only the performance on D_t matters, CT again compares favorably against the best UDA method, *i.e.* GSFDA. CT is also better than KDDE and MultiT. As for the UDE setting, the lower performance of MultiT than KDDE and CT (71.94 versus 74.37 and 74.89) confirms our hypothesis that the two teacher networks shall not be treated equally in the knowledge distillation process. Given DDC as \mathcal{N}_t , CT outperforms KDDE by 0.52% (72.47 \rightarrow 72.99). When using CDAN as \mathcal{N}_t , a larger gain of 1.36% (72.00 \rightarrow 73.36) is obtained on Office-Home. While the number might appear to be small, this is typically considered significant in the literature, see [16, 39, 43], due to the challenging nature of the task.

For a better understanding of how the student network is affected by the different knowledge distillation methods, *i.e.* KDDE, MultiT and kdCT, we group all test samples w.r.t. to the prediction (in)consistency between the two teacher networks. In particular, depending on whether the predictions of \mathcal{N}_s and \mathcal{N}_t are consistent (=) or inconsistent (\neq), samples are exclusively grouped. The fine-grained result is shown in Tab. 2. We can mostly attribute the success of kdCT to its superior performance on the inconsistent group, which confirms the effectiveness of compensation mechanism from CT. As Fig. 3 shows, the activated regions w.r.t. kdCT is more precise than the others. Both quantitative and qualitative results justify the efficacy of CT.

4.1.3 Results on DomainNet As DomainNet is much larger than Office-Home in terms of classes and samples, we are only able to train the following UDA methods, *i.e.* CDAN, DANN and DDC. As Tab. 1 shows, using either DDC or CDAN as \mathcal{N}_t , our CT method again achieves the best performance on D_s , D_t and D_{s+t} .

4.1.4 Ablation Study We choose Office-Home for ablation study, simply because the set is more computationally friendly than DomainNet.

The influence of kdCT and miCT. As shown in Tab. 3, kdCT is better than miCT when they are used alone. Their joint use is recommended for the image classification task. The lower performance of miCT is because we train on mixup samples exclusively, without using original samples. Similar to a standard mixup, mixup samples shall not be used alone.

Table 1. Multi-class image classification on Office-Home and DomainNet in the UDA/UDE setting. Cells with n.a. indicate that running the specific methods is beyond our computational capacity. Note that we follow the data split of KDDE where 50% of the source/target-domain samples are held out for testing. So the performance of the existing UDA methods is lower than that reported in their original papers.

| Method | OfficeHome | | | DomainNet | | |
|--|--------------|--------------|--------------|--------------|--------------|--------------|
| | D_s | D_t | D_{s+t} | D_s | D_t | D_{s+t} |
| ResNet-50 (\mathcal{N}_s) | 82.43 | 57.84 | 70.13 | 74.59 | 41.49 | 58.04 |
| <i>Choice of \mathcal{N}_t:</i> | | | | | | |
| CDAN [14] | 80.36 | 61.57 | 70.96 | 69.73 | 45.21 | 57.47 |
| DANN [6] | 81.36 | 60.65 | 71.01 | 67.37 | 44.53 | 56.95 |
| DDC [33] | 82.35 | 60.51 | 71.43 | 72.44 | 46.20 | 59.32 |
| DAAN [43] | 82.38 | 60.84 | 71.62 | n.a. | n.a. | n.a. |
| SRDC [31] | 78.68 | 65.30 | 71.99 | n.a. | n.a. | n.a. |
| GSFDA [39] | 79.90 | 66.53 | 73.22 | n.a. | n.a. | n.a. |
| <i>DDC as \mathcal{N}_t:</i> | | | | | | |
| KDDE [37] | 82.74 | 62.19 | 72.47 | 73.78 | 48.04 | 60.91 |
| PDA [16] | 76.90 | 54.01 | 65.46 | n.a. | n.a. | n.a. |
| CT | 82.92 | 63.06 | 72.99 | 74.63 | 48.42 | 61.53 |
| <i>CDAN as \mathcal{N}_t:</i> | | | | | | |
| KDDE | 81.03 | 62.96 | 72.00 | 72.98 | 47.65 | 60.32 |
| PDA | 78.44 | 57.65 | 68.04 | n.a. | n.a. | n.a. |
| CT | 82.17 | 64.55 | 73.36 | 73.26 | 49.33 | 61.29 |
| <i>SRDC as \mathcal{N}_t:</i> | | | | | | |
| MultiT [42] | 82.23 | 61.66 | 71.94 | n.a. | n.a. | n.a. |
| KDDE | 81.54 | 67.20 | 74.37 | n.a. | n.a. | n.a. |
| CT | 82.32 | 67.45 | 74.89 | n.a. | n.a. | n.a. |

The influence of γ . Tab. 4 reports the performance of kdCT given γ specified in varied manners. The stochastic strategy with $\gamma \sim Beta(10, 1)$ leads to the best performance on the expanded domain. In particular, we also tried fixing γ to 0.909, which is the expectation value of $Beta(10, 1)$, see Fig. 4. Comparing the first row and the last second row in Tab. 4, we observe that using the fixed value results in lower performance consistently on D_s (82.81 versus 82.85), D_t (61.67 versus 62.42) and D_{s+t} (72.24 versus 72.63). The results justify the benefit of using γ in a stochastic manner.

4.2 Task 2. Driving Scene Segmentation

4.2.1 Experimental Setup We follow the setup of [25], using Cityscapes [4] as D_s and ACDC [25] as D_t . Both datasets have pixel-level ground truth w.r.t. 19 traffic-related labels such as bicycle, road and sidewalk. Different from Cityscapes consisting of normal lighttime driving scenes, ACDC have four adverse conditions, *i.e.* fog, nighttime, rain and snow, see Fig. 5. For both datasets, we adopt their official data splits, *i.e.* 2,975 training and 500 test images in Cityscapes and 1,600 training and 406 test images in ACDC.

Table 2. Performance of different methods on two groups of test samples. Given a specific test set, say D_s , it can be divided into two disjoint subsets, *i.e.* consistent and inconsistent, where each sample x in the consistent set has $\mathcal{N}_s(x) == \mathcal{N}_t(x)$, while each sample in the inconsistent set has $\mathcal{N}_s(x) \neq \mathcal{N}_t(x)$. The classification accuracy score is calculated per subset. The gain of kdCT against KDDE and MultiT is mostly attributed to the method’s better performance on the inconsistent group.

| Task | D_s | | D_t | | D_{s+t} | |
|-----------------|-------|-------|-------|-------|-----------|-------|
| R→P | = | ≠ | = | ≠ | = | ≠ |
| \mathcal{N}_s | 90.00 | 42.75 | 87.54 | 21.88 | 88.80 | 30.20 |
| \mathcal{N}_t | 90.00 | 30.07 | 87.54 | 48.31 | 88.80 | 41.04 |
| KDDE | 88.96 | 42.39 | 87.32 | 51.20 | 88.16 | 47.69 |
| MultiT | 88.96 | 44.57 | 86.61 | 41.59 | 87.81 | 42.77 |
| kdCT | 89.53 | 47.46 | 87.54 | 52.88 | 88.56 | 50.72 |
| Task | D_s | | D_t | | D_{s+t} | |
| A→C | = | ≠ | = | ≠ | = | ≠ |
| \mathcal{N}_s | 85.19 | 43.30 | 66.50 | 16.13 | 74.41 | 22.90 |
| \mathcal{N}_t | 85.19 | 18.30 | 66.50 | 27.61 | 74.41 | 25.31 |
| KDDE | 81.90 | 36.14 | 65.13 | 29.99 | 72.26 | 31.52 |
| MultiT | 83.87 | 40.19 | 65.45 | 27.51 | 73.25 | 30.67 |
| kdCT | 82.98 | 43.30 | 66.75 | 32.78 | 73.62 | 35.40 |

Table 3. Ablation Study of Co-Teaching on Office-Home.

| kdCT | miCT | D_s | D_t | D_{s+t} |
|---|------|--------------|--------------|--------------|
| <i>DDC as \mathcal{N}_t</i> | | | | |
| ✓ | | 82.85 | 62.42 | 72.63 |
| | ✓ | 80.32 | 61.90 | 71.11 |
| ✓ | ✓ | 82.92 | 63.06 | 72.99 |
| <i>SRDC as \mathcal{N}_t</i> | | | | |
| ✓ | | 82.52 | 67.19 | 74.86 |
| | ✓ | 77.46 | 63.85 | 70.65 |
| ✓ | ✓ | 82.32 | 67.45 | 74.89 |

Competitor methods. We again compare with KDDE [37]. Our choice of \mathcal{N}_s is DeepLabv2 [3] with ResNet-101 as its backbone, as has been used in the previous work [25]. As for \mathcal{N}_t , we adopt the classic AdaSegNet [32] and the more recent FDA [41], which is found to be the most effective on ACDC [25].

Details of Implementation. Following [3], we adopt SGD with an initial learning rate of 0.001, a momentum of 0.9, and a weight decay of 0.0005. We train 75000 iterations with batch size 1. Previous work on semantic image segmentation [20] reports the Mixup technique has an adverse effect on the performance, which is also observed in our preliminary experiment on driving scene segmentation, we therefore uses CT without miCT for this task.

Performance metric. We report IoU per class, and mean IoU (mIoU) for measuring the overall performance.

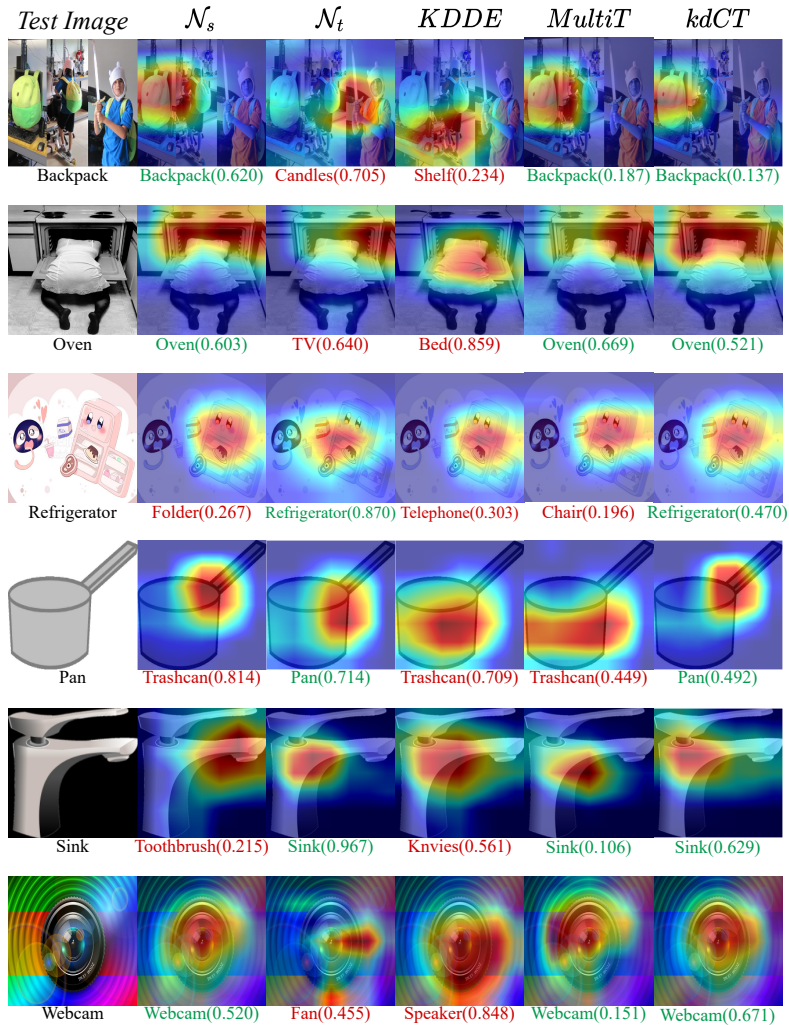


Fig. 3. Grad-CAM [28] visualization of ResNet-50 trained by different methods. The top three rows are from the source domain (*Art*), while the bottom three rows are from the target domain (*Clipart*). Text under each heatmap is a prediction with its score.

4.2.2 Results On the source domain D_s , we observe that the performance of the AdaSegNet and FDA decreases in 6, which confirms the necessity of the UDE for semantic segmentation. Two-stage methods can alleviate the decline, and CT outperforms KDDE. Under the UDA setting, CT boosts both UDA methods and achieves the best performance on the target domain D_t . More visually in 5, for the adverse conditions, we can obviously observe that CT can produce more accurate segmentation and improve the generalization, such as eliminating the

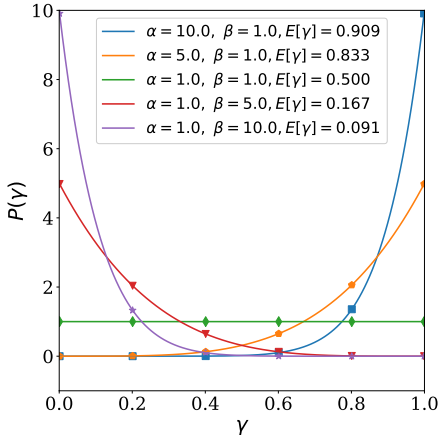


Fig. 4. Beta distributions parameterized by different α and β . $E(\gamma)$ represents the distribution expectation.

Table 4. Evaluating the influence of γ on kdCT. Best performance is obtained by sampling γ from $Beta(10, 1)$, which has an expectation of 0.909. Fixing γ to 0.909 results in lower performance consistently on D_s , D_t and D_{s+t} . Choice of \mathcal{N}_t : DDC. Tested on Office-Home.

| | D_s | D_t | D_{s+t} |
|--|--------------|--------------|--------------|
| <hr/> | | | |
| (α, β) of the beta distribution | | | |
| 10, 1 | 82.85 | 62.42 | 72.63 |
| 5, 1 | 82.84 | 62.02 | 72.43 |
| 1, 1 | 82.86 | 61.54 | 72.20 |
| 1, 5 | 82.78 | 60.61 | 71.70 |
| 1, 10 | 82.65 | 60.61 | 71.63 |
| <hr/> | | | |
| <i>Fixed</i> | | | |
| 0.5 | 82.75 | 61.41 | 72.08 |
| 0.909 | 82.81 | 61.67 | 72.24 |
| 1 | 82.74 | 62.19 | 72.47 |

misclassification of the sky into buildings. On the expanded domain, CT achieves the best performance on the most categories in 6 and CT(FDA) achieves the best average performance for UDE. This demonstrates our method’s applicability to cross-condition driving scene segmentation. Tab. 5 shows pixel-level accuracy. CT better handles pixels that have inconsistent predictions by \mathcal{N}_s and \mathcal{N}_t .

Table 5. Pixel-level classification accuracy. CT performs the best on samples for which \mathcal{N}_s and \mathcal{N}_t disagrees.

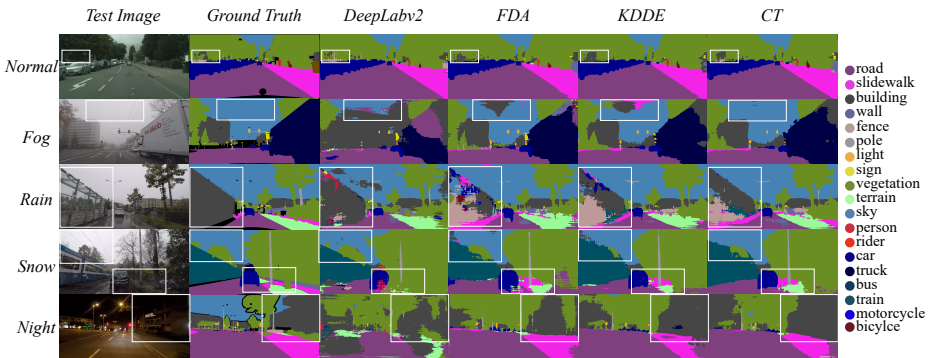
| Method | D_s | | D_t | | D_{s+t} | |
|------------------------------|-------|------|-------|-------|-----------|-------|
| | = | ≠ | = | ≠ | = | ≠ |
| DeepLabv2 as \mathcal{N}_s | 95.99 | 3.06 | 86.31 | 9.92 | 92.20 | 5.74 |
| FDA as \mathcal{N}_t | 95.99 | 2.55 | 86.31 | 21.30 | 92.20 | 9.89 |
| CT (FDA) | 95.29 | 3.49 | 86.66 | 26.13 | 91.91 | 12.35 |

5 Summary and Conclusions

We have presented Co-Teaching (CT) as new method for both UDA and UDE. Our multi-class image classification experiments on two public benchmarks, *i.e.* Office-Home and DomainNet, and semantic image segmentation experiments on another two public sets, *i.e.* Cityscapes and ACDC, support our conclusions as follows. Due to the existence of cross-domain visual ambiguity, a domain-specific model is not universally applicable to handle samples from its targeted domain. With its ability to resolve such visual ambiguity, CT beats strong baselines on

Table 6. UDA/UDE performance of driving scene segmentation. Metric: IoU.

| Method | road | sidewalk | build. | wall | fence | pole | light | sign | veget. | terrain | sky | person | rider | car | truck | bus | train | motor. | bicycle | mIoU |
|--|--------------|--------------|--------------|--------------|--------------|--------------|--------------|--------------|--------------|--------------|--------------|--------------|--------------|--------------|--------------|--------------|--------------|--------------|--------------|--------------|
| <i>Tested on the source domain D_s, i.e. Cityscapes:</i> | | | | | | | | | | | | | | | | | | | | |
| DeepLabv2 | 96.22 | 73.58 | 87.39 | 42.65 | 40.08 | 40.35 | 45.01 | 60.11 | 88.17 | 49.38 | 88.95 | 67.67 | 47.61 | 90.74 | 61.81 | 66.51 | 43.66 | 50.57 | 63.05 | 63.34 |
| AdaSegNet | 96.20 | 72.73 | 87.53 | 32.48 | 41.48 | 40.82 | 41.06 | 60.01 | 87.30 | 41.70 | 90.99 | 67.22 | 48.21 | 89.83 | 68.98 | 62.07 | 31.05 | 50.39 | 62.14 | 61.69 |
| FDA | 95.99 | 71.38 | 86.37 | 43.45 | 37.29 | 38.67 | 41.82 | 57.03 | 86.69 | 48.03 | 88.65 | 64.97 | 44.05 | 88.56 | 69.24 | 58.28 | 30.21 | 45.60 | 61.46 | 60.93 |
| AdaSegNet as N_t : | | | | | | | | | | | | | | | | | | | | |
| KDDE | 96.20 | 72.94 | 87.30 | 36.50 | 40.16 | 40.26 | 40.12 | 58.78 | 87.65 | 45.05 | 90.24 | 66.64 | 47.75 | 90.63 | 69.72 | 64.40 | 31.27 | 49.66 | 62.33 | 61.98 |
| CT | 96.15 | 73.47 | 87.39 | 36.69 | 42.00 | 41.77 | 41.60 | 59.49 | 87.64 | 41.57 | 90.11 | 67.39 | 47.57 | 90.46 | 69.11 | 63.71 | 48.76 | 44.50 | 62.29 | 62.72 |
| FDA as N_t : | | | | | | | | | | | | | | | | | | | | |
| KDDE | 96.20 | 73.69 | 87.09 | 43.19 | 41.32 | 39.72 | 37.16 | 57.19 | 87.73 | 47.30 | 89.99 | 66.84 | 47.22 | 90.34 | 67.56 | 64.73 | 35.95 | 45.08 | 61.46 | 62.09 |
| CT | 95.97 | 73.58 | 87.09 | 37.59 | 42.79 | 40.73 | 39.55 | 59.28 | 87.41 | 42.91 | 90.38 | 66.34 | 47.81 | 90.40 | 72.15 | 61.20 | 37.34 | 47.06 | 61.78 | 62.18 |
| <i>Tested on the target domain D_t, i.e. ACDC:</i> | | | | | | | | | | | | | | | | | | | | |
| DeepLabv2 | 59.60 | 20.09 | 43.67 | 10.16 | 12.90 | 22.86 | 39.94 | 34.11 | 66.24 | 17.00 | 58.13 | 17.31 | 8.20 | 46.04 | 28.60 | 21.61 | 32.88 | 22.89 | 15.79 | 30.25 |
| AdaSegNet | 49.36 | 30.92 | 68.16 | 24.50 | 22.09 | 31.33 | 51.08 | 38.85 | 55.53 | 26.40 | 34.39 | 28.18 | 12.58 | 64.73 | 36.94 | 40.10 | 50.11 | 27.02 | 22.56 | 38.20 |
| FDA | 75.00 | 38.31 | 61.23 | 22.10 | 23.75 | 30.26 | 47.74 | 37.00 | 66.35 | 25.73 | 68.17 | 38.54 | 13.31 | 65.37 | 33.03 | 52.77 | 44.34 | 16.84 | 21.32 | 41.11 |
| AdaSegNet as N_t : | | | | | | | | | | | | | | | | | | | | |
| KDDE | 59.45 | 29.49 | 69.18 | 23.45 | 22.17 | 31.74 | 52.88 | 39.40 | 67.02 | 26.02 | 53.10 | 30.82 | 10.02 | 52.93 | 38.28 | 45.06 | 51.22 | 23.83 | 23.80 | 39.47 |
| CT | 64.25 | 27.03 | 68.58 | 23.53 | 23.02 | 31.28 | 53.96 | 39.96 | 67.82 | 27.10 | 62.96 | 32.06 | 12.09 | 69.17 | 39.19 | 36.27 | 49.04 | 21.99 | 27.45 | 40.88 |
| FDA as N_t : | | | | | | | | | | | | | | | | | | | | |
| KDDE | 76.35 | 33.10 | 62.02 | 18.95 | 25.15 | 30.49 | 52.94 | 35.98 | 68.74 | 25.96 | 71.15 | 31.02 | 10.59 | 70.99 | 30.92 | 48.93 | 50.32 | 26.86 | 25.26 | 41.83 |
| CT | 77.72 | 35.76 | 60.12 | 15.86 | 24.34 | 30.29 | 51.46 | 38.08 | 70.15 | 26.48 | 74.38 | 35.80 | 13.48 | 69.74 | 40.50 | 48.28 | 48.81 | 28.55 | 22.83 | 42.77 |
| <i>Tested on the expanded domain D_{s+t}, i.e. Cityscapes + ACDC:</i> | | | | | | | | | | | | | | | | | | | | |
| DeepLabv2 | 84.31 | 48.39 | 63.59 | 20.35 | 23.24 | 34.22 | 42.96 | 52.54 | 75.83 | 25.66 | 61.98 | 56.57 | 45.45 | 78.06 | 42.97 | 45.79 | 34.24 | 41.97 | 58.46 | 49.29 |
| AdaSegNet | 75.53 | 52.73 | 79.63 | 27.38 | 30.04 | 37.48 | 45.45 | 53.68 | 75.07 | 32.78 | 41.38 | 60.69 | 46.21 | 83.92 | 50.60 | 51.65 | 47.12 | 42.72 | 58.18 | 52.22 |
| FDA | 88.95 | 54.76 | 75.28 | 29.32 | 28.56 | 35.68 | 44.29 | 51.51 | 74.97 | 34.28 | 70.70 | 62.17 | 42.86 | 83.31 | 47.17 | 55.61 | 42.11 | 35.12 | 56.58 | 53.33 |
| AdaSegNet as N_t : | | | | | | | | | | | | | | | | | | | | |
| KDDE | 81.63 | 52.03 | 79.83 | 28.31 | 29.40 | 37.31 | 45.64 | 53.13 | 75.58 | 34.03 | 57.68 | 61.14 | 45.27 | 80.39 | 51.98 | 55.49 | 48.35 | 41.55 | 58.81 | 53.55 |
| CT | 84.07 | 51.45 | 79.54 | 28.53 | 30.65 | 38.20 | 46.87 | 53.77 | 76.08 | 33.34 | 66.32 | 62.23 | 45.24 | 85.74 | 52.59 | 50.77 | 49.00 | 37.50 | 59.18 | 54.27 |
| FDA as N_t : | | | | | | | | | | | | | | | | | | | | |
| KDDE | 89.59 | 53.08 | 75.84 | 27.35 | 31.23 | 36.52 | 44.11 | 51.18 | 76.96 | 34.99 | 73.44 | 62.27 | 45.25 | 86.08 | 44.60 | 56.16 | 48.21 | 39.07 | 57.35 | 54.38 |
| CT | 89.99 | 54.79 | 74.59 | 23.48 | 31.28 | 37.14 | 44.67 | 53.32 | 77.80 | 33.68 | 76.34 | 63.01 | 46.26 | 85.81 | 54.50 | 54.89 | 47.20 | 41.32 | 57.55 | 55.14 |

**Fig. 5.** Qualitative results of driving scene segmentation. The first row is from D_s (normal condition in the sunlight), while the other rows are from D_t (adverse conditions in the nighttime, fog, snow and rain). Important difference between the results is marked out by white bounding boxes.

UDA, *i.e.* GSFDA for image classification and FDA for driving scene segmentation. CT is also better than the prior art on UDE, *i.e.* KDDE, for both tasks.

References

1. Belal, A., Kiran, M., Dolz, J., Blais-Morin, L.A., Granger, E., et al.: Knowledge distillation methods for efficient unsupervised adaptation across multiple domains. *Image and Vision Computing* **108**, 104096 (2021) [4](#)
2. Ben-David, S., Blitzer, J., Crammer, K., Kulesza, A., Pereira, F., Vaughan, J.W.: A theory of learning from different domains. *Machine learning* **79**(1), 151–175 (2010) [1](#)
3. Chen, L.C., Papandreou, G., Kokkinos, I., Murphy, K., Yuille, A.L.: Deeplab: Semantic image segmentation with deep convolutional nets, atrous convolution, and fully connected crfs. *IEEE transactions on pattern analysis and machine intelligence* **40**(4), 834–848 (2017) [7](#), [11](#)
4. Cordts, M., Omran, M., Ramos, S., Rehfeld, T., Enzweiler, M., Benenson, R., Franke, U., Roth, S., Schiele, B.: The cityscapes dataset for semantic urban scene understanding. In: *CVPR* (2016) [3](#), [10](#)
5. Fawzi, A., Moosavi-Dezfooli, S.M., Frossard, P.: Robustness of classifiers: from adversarial to random noise. In: *NIPS* (2016) [7](#)
6. Ganin, Y., Ustinova, E., Ajakan, H., Germain, P., Larochelle, H., Laviolette, F., March, M., Lempitsky, V.: Domain-adversarial training of neural networks. *JMLR* **17**(59), 1–35 (2016) [3](#), [8](#), [10](#)
7. Han, B., Yao, Q., Yu, X., Niu, G., Xu, M., Hu, W., Tsang, I., Sugiyama, M.: Co-teaching: Robust training of deep neural networks with extremely noisy labels. *NIPS* **31** (2018) [4](#)
8. He, K., Zhang, X., Ren, S., Sun, J.: Deep residual learning for image recognition. In: *CVPR*. pp. 770–778 (2016) [7](#)
9. He, Z., Rakin, A.S., Fan, D.: Parametric noise injection: Trainable randomness to improve deep neural network robustness against adversarial attack. In: *CVPR*. pp. 588–597 (2019) [7](#)
10. Hoffman, J., Tzeng, E., Park, T., Zhu, J.Y., Isola, P., Saenko, K., Efros, A., Darrell, T.: Cycada: Cycle-consistent adversarial domain adaptation. In: *ICML*. pp. 1989–1998. PMLR (2018) [3](#)
11. Kang, G., Jiang, L., Yang, Y., Hauptmann, A.G.: Contrastive adaptation network for unsupervised domain adaptation. In: *CVPR*. pp. 4893–4902 (2019) [3](#)
12. Li, S., Liu, C.H., Xie, B., Su, L., Ding, Z., Huang, G.: Joint adversarial domain adaptation. In: *ACMMM* (2019) [3](#)
13. Lin, Y., Wu, Y., Yan, C., Xu, M., Yang, Y.: Unsupervised person re-identification via cross-camera similarity exploration. *IEEE Transactions on Image Processing* **29**, 5481–5490 (2020) [1](#)
14. Long, M., Cao, Z., Wang, J., Jordan, M.I.: Conditional adversarial domain adaptation. In: *NIPS* (2018) [3](#), [8](#), [10](#)
15. Long, M., Zhu, H., Wang, J., Jordan, M.I.: Deep transfer learning with joint adaptation networks. In: *ICML* (2017) [3](#)
16. Lv, F., Liang, J., Gong, K., Li, S., Liu, C.H., Li, H., Liu, D., Wang, G.: Pareto domain adaptation. In: *NIPS* (2021) [4](#), [8](#), [9](#), [10](#)
17. Malach, E., Shalev-Shwartz, S.: “Decoupling” when to update” from” how to update”. *NIPS* **30** (2017) [4](#)
18. Mansour, Y., Mohri, M., Rostamizadeh, A.: Domain adaptation: Learning bounds and algorithms. In: *COLT* (2009) [1](#)
19. Pan, S.J., Yang, Q.: A survey on transfer learning. *IEEE Transactions on knowledge and data engineering* **22**(10), 1345–1359 (2009) [1](#)

20. Panfilov, E., Tiulpin, A., Klein, S., Nieminen, M.T., Saarakkala, S.: Improving robustness of deep learning based knee mri segmentation: Mixup and adversarial domain adaptation. In: ICCV Workshop. pp. 0–0 (2019) [11](#)
21. Peng, X., Bai, Q., Xia, X., Huang, Z., Saenko, K., Wang, B.: Moment matching for multi-source domain adaptation. In: ICCV (2019) [1](#), [3](#), [8](#)
22. Roy, S., Krivosheev, E., Zhong, Z., Sebe, N., Ricci, E.: Curriculum graph co-teaching for multi-target domain adaptation. In: Proceedings of the IEEE/CVF Conference on Computer Vision and Pattern Recognition (2021) [4](#)
23. Saito, K., Watanabe, K., Ushiku, Y., Harada, T.: Maximum classifier discrepancy for unsupervised domain adaptation. In: CVPR (2018) [3](#)
24. Sakaridis, C., Dai, D., Van Gool, L.: Map-guided curriculum domain adaptation and uncertainty-aware evaluation for semantic nighttime image segmentation. IEEE Transactions on Pattern Analysis and Machine Intelligence pp. 1–1 (2020) [1](#)
25. Sakaridis, C., Dai, D., Van Gool, L.: ACDC: The adverse conditions dataset with correspondences for semantic driving scene understanding. In: ICCV (October 2021) [1](#), [3](#), [10](#), [11](#)
26. Sebastian Ruder, Parsa Ghaffari, J.G.B.: Knowledge adaptation: Teaching to adapt. In: ICLR (2017) [4](#)
27. Seeböck, P., Romo-Bucheli, D., Waldstein, S., Bogunovic, H., Orlando, J.I., Gerasdas, B.S., Langs, G., Schmidt-Erfurth, U.: Using cyclegans for effectively reducing image variability across oct devices and improving retinal fluid segmentation. In: ISBI. pp. 605–609. IEEE (2019) [1](#)
28. Selvaraju, R.R., Cogswell, M., Das, A., Vedantam, R., Parikh, D., Batra, D.: Grad-cam: Visual explanations from deep networks via gradient-based localization. In: ICCV (2017) [12](#)
29. Srivastava, N., Hinton, G., Krizhevsky, A., Sutskever, I., Salakhutdinov, R.: Dropout: a simple way to prevent neural networks from overfitting. The journal of machine learning research **15**(1), 1929–1958 (2014) [7](#)
30. Sun, B., Saenko, K.: Deep CORAL: Correlation Alignment for Deep Domain Adaptation. In: ECCV Workshop (2016) [3](#)
31. Tang, H., Chen, K., Jia, K.: Unsupervised domain adaptation via structurally regularized deep clustering. In: CVPR. pp. 8725–8735 (2020) [1](#), [3](#), [8](#), [10](#)
32. Tsai, Y.H., Hung, W.C., Schuler, S., Sohn, K., Yang, M.H., Chandraker, M.: Learning to adapt structured output space for semantic segmentation. In: CVPR. pp. 7472–7481 (2018) [3](#), [11](#)
33. Tzeng, E., Hoffman, J., Zhang, N., Saenko, K., Darrell, T.: Deep domain confusion: Maximizing for domain invariance. ArXiv [abs/1412.3474](#) (2014) [3](#), [8](#), [10](#)
34. Valada, A., Vertens, J., Dhall, A., Burgard, W.: Adapnet: Adaptive semantic segmentation in adverse environmental conditions. In: ICRA. pp. 4644–4651. IEEE (2017) [1](#)
35. Venkateswara, H., Eusebio, J., Chakraborty, S., Panchanathan, S.: Deep hashing network for unsupervised domain adaptation. In: CVPR (2017) [1](#), [2](#), [3](#), [8](#)
36. Vu, T.H., Jain, H., Bucher, M., Cord, M., Perez, P.: Advent: Adversarial entropy minimization for domain adaptation in semantic segmentation. In: Proceedings of the IEEE/CVF Conference on Computer Vision and Pattern Recognition (CVPR) (June 2019) [3](#)
37. Wang, J., Tian, K., Ding, D., Yang, G., Li, X.: Unsupervised domain expansion for visual categorization. ACM Trans. Multimedia Comput. Commun. Appl. **17**(4) (Nov 2021) [2](#), [3](#), [4](#), [5](#), [8](#), [10](#), [11](#)

38. Wu, Z., Han, X., Lin, Y.L., Uzunbas, M.G., Goldstein, T., Lim, S.N., Davis, L.S.: Dcan: Dual channel-wise alignment networks for unsupervised scene adaptation. In: ECCV. pp. 518–534 (2018) **3**
39. Yang, S., Wang, Y., van de Weijer, J., Herranz, L., Jui, S.: Generalized source-free domain adaptation. In: ICCV. pp. 8978–8987 (2021) **2, 4, 8, 9, 10**
40. Yang, S., Zhou, X., Wang, J., Xie, G., Lv, C., Gao, P., Lv, B.: Unsupervised domain adaptation for cross-device oct lesion detection via learning adaptive features. In: ISBI. pp. 1570–1573 (2020) **1**
41. Yang, Y., Soatto, S.: Fda: Fourier domain adaptation for semantic segmentation. In: CVPR. pp. 4085–4095 (2020) **1, 3, 8, 11**
42. You, S., Xu, C., Xu, C., Tao, D.: Learning from multiple teacher networks. In: SIGKDD. pp. 1285–1294 (2017) **4, 8, 10**
43. Yu, C., Wang, J., Chen, Y., Huang, M.: Transfer learning with dynamic adversarial adaptation network. In: ICDM (2019) **3, 8, 9, 10**
44. Zhang, H., Cisse, M., Dauphin, Y.N., Lopez-Paz, D.: mixup: Beyond empirical risk minimization. In: ICLR (2018) **7**
45. Zhang, M., Liu, K., Li, Y., Guo, S., Duan, H., Long, Y., Jin, Y.: Unsupervised domain adaptation for person re-identification via heterogeneous graph alignment. In: AAAI. vol. 35, pp. 3360–3368 (2021) **1**